

Original Article

Real-Time Masked Face Recognition System Using Deep Learning Based Graph Convolutional Network with Heuristic Search Algorithm

D. Gayathry¹, R. Latha²

¹Department of Computer Science, St. Peter's Institute of Higher Education and Research, Chennai, Tamil Nadu, India.

²Department of Computer Science & Applications, St. Peter's Institute of Higher Education and Research, Chennai, Tamil Nadu, India.

¹Corresponding Author : gaya200689@gmail.com

Received: 16 October 2025

Revised: 17 November 2025

Accepted: 16 December 2025

Published: 27 December 2025

Abstract - With the COVID-19 pandemic worldwide, utilising face masks has become a significant part of everyone's life, and everybody uses masks to avert the spread of the infection during the epidemic. This nearly makes conventional facial recognition technology ineffectual in numerous situations, such as community visit check-ins, face authentication, and security checks. The face recognition-based security method, however, avoids redundant contact, making it much more secure than the previous one. But such methods require using an image of the complete face to do recognition successfully. So, it is vital to increase the performance of current face detection methods on masked faces. Most current cutting-edge face recognition methods rely on Deep Learning (DL), which is heavily dependent on a large number of training samples. This paper proposes a Masked Face Recognition System Using Graph Convolutional Network with Metaheuristic Optimisation Algorithm (MFRS-GCNMOA) technique. The aim is to create an accurate model for detecting masked faces in real-time for enhanced security and surveillance applications. At first, the image pre-processing phase employs the Wiener Filtering (WF) technique for improving image quality. For effective feature extraction, the MFRS-GCNMOA technique utilizes the ResNet-152 method to capture facial patterns from image data. Furthermore, the Graph Convolutional Network (GCN) technique is employed for the classification process. To improve classification performance, the parameter tuning process is achieved by using the Starfish Optimisation Algorithm (SFOA) technique. Finally, the faster-RCNN method is used for face mask detection. To show an improved performance of the presented MFRS-GCNMOA technique, a complete experimental study is conducted under the face mask detection dataset. The comparison assessment of the MFRS-GCNMOA technique portrayed a superior accuracy value of 98.49% over existing models.

Keywords - Masked Face Recognition; Graph Convolutional Network; Starfish Optimisation Algorithm; Wiener Filtering; Deep Learning.

1. Introduction

Face Recognition (FR) methods usually examine main facial characteristics such as the mouth, eyes, and nose on uncovered faces. Different circumstances and events require individuals to wear masks that partly obscure or conceal their characteristics [1]. Usual scenarios include laboratories, excessive pollution, medicinal procedures, and pandemics. The WHO suggested wearing Face Masks (FM) and maintaining physical distance as effective methods to safeguard against COVID-19 [2]. All states globally made masks mandatory, creating a need to study and understand the implementation of FR methods with masked faces [3]. Applying these protection regulations is an essential task for recent security measures, which rely on facial detection technologies. Current approaches aim to detect if a face is closed, particularly in the context of detecting an FM [4].

While protective life spans are significant, it becomes crucial to verify that people are wearing masks. Detection becomes difficult due to people wearing masks in areas such as immigration and premises access control [5]. Masks obscure an essential part of the face; therefore, wearing masks may have a significant impact on recognising an individual's identity [6]. This problem has generated anxieties in various industries and regions that require an individual's identification, such as the verification needed for attendance registration in businesses or unlocking a phone, and several personal security schemes [7].

Utilising typical methods of unlocking, namely fingerprints and passwords, can propagate the infection. Therefore, FR is the optimum approach to unlock or authenticate security systems to restrict the transmission risk



[8]. Technical efforts to address the epidemic's expansion are underway. To fight this pandemic, scholars are resorting to Artificial Intelligence (AI), especially DL, which has already demonstrated enhanced execution in the medical field and can discover patterns in highly complex databases [9]. More particularly, DL has recently made significant developments in different fields, involving picture categorisation, segmentation, detection, identification, and object finding [10]. Accordingly, it was substantial to utilise these abilities to fight the epidemic. In the COVID-19 pandemic, AI methods helped in forecasting the spread of diseases or the virus, leading to warnings and appropriate preventive activities [11]. The Deep Neural Network (DNN) approach provides a different method that aids in coronavirus classification, image processing, and detection. Convolutional Neural Network (CNN) is among the essential networks.

This paper proposes a Masked Face Recognition System Using Graph Convolutional Network with Metaheuristic Optimisation Algorithm (MFRS-GCNMOA) technique. The aim is to create an accurate model for detecting masked faces in real-time for enhanced security and surveillance applications. At first, the image pre-processing phase employs the Wiener Filtering (WF) technique for improving image quality. For effective feature extraction, the MFRS-GCNMOA technique utilizes the ResNet-152 method to capture facial patterns from image data. Furthermore, the Graph Convolutional Network (GCN) technique is employed for the classification process. To improve classification performance, the parameter tuning process is achieved by using the Starfish Optimisation Algorithm (SFOA) technique. Finally, the faster-RCNN method is used for face mask detection. To show an improved performance of the presented MFRS-GCNMOA technique, a complete experimental study is conducted under the face mask detection dataset.

- The WF is utilized for effectively mitigating image noise and improving quality in the pre-processing phase, enabling more precise and reliable recognition of facial features. The process also contributes to an enhanced performance in masked face detection.
- The ResNet-152 is employed for extracting intrinsic and discriminative facial patterns from masked face images, thus enhancing feature representation. The model also improved recognition accuracy and strengthened the performance of the method in real-time masked face detection.
- The GCN is implemented for performing structured learning between facial features. The model also improved the ability of the technique in capturing spatial and relational data, thus enhancing classification accuracy and strengthening overall performance in masked face recognition tasks.
- The SFOA methodology is employed for fine-tuning the parameters of GCN, enhancing classification performance, reliability, optimizing recognition accuracy, and ensuring the model effectively adapts to

discrepancies in masked face images.

- The novelty of the MFRS-GCNMOA approach is in the integrated ResNet-152, GCN, and SFOA models, while also incorporating Faster-RCNN for accurate mask detection, thus presenting a novel, comprehensive, and real-time solution that significantly improves recognition performance under masked conditions.

2. Related Works

Tarnpradab et al. [3] introduced a web-driven application system for accomplishing three significant challenges. Currently, it is essential to recognise whether a person is at the location to wear the FM. At last, definitely modernise the recognition method with the very current user record, with an accessible port from the current web page. The essential method for detecting and recognising is the CNN technique. In [13], a Hybrid Flame-Sailfish Optimisation (HFSO)-Driven DL structure is presented. It integrates the feature extractor abilities of ResNet-50 with the efficacy of MobileNet-v2. This method optimises critical limits, namely learning rates and detection thresholds. Therefore, the approach can make full use of computing ability and yet operate in actual devices with inadequate resources. This structure is consistent and user-friendly for identifying individuals wearing FMs in various circumstances.

In [14], a novel method of utilising sparse representation and a DL approach, named Sparse Representation driven classification combined with a customised CNN (Sparse CNN), is suggested for enhancing the solution of wearing mask FR. This approach uses CNN for feature extraction and Sparse Representation Driven Classification (SRC) to improve precision. By integrating both methods, this approach leverages consistency against interference and extreme precision in recognising the noise problem of the sparse model, while using CNNs to minimise the arrangement problem. TUN and Myat [15] presented a DL-driven technique for actual FM recognition to help in applying mask-wearing procedures.

Primarily, faces are localised in the input picture or video stream employing a presented FR method. Al-Dmour et al. [16] introduced a new DL-driven approach to detect and mask FR, determine independence, and assess whether the face is appropriately masked, utilising different face picture information. This method was trained employing a CNN with early stopping and cross-validation. Binary classification is used to distinguish unmasked and masked faces. Therefore, a multi-class method was aimed at classifying the FM images into three labels: non-masked, correctly masked, and incorrectly masked. Kumar [17] suggested a DL technique for masked face detection. In surveillance settings, complete transparency of facial regions is standard, and criminals often commit crimes while hiding their faces with masks. Eman et al. [18] introduced a new model that integrates DL-driven with a Robust Principal Component Analysis (RPCA) method.

Particularly, utilise pretrained SSD-MobileNetv2 to identify the attendance and mask position on a face, and oval FR and landmark for identifying important face characteristics. This approach also uses RPCA to distinguish non-occluded and occluded parts of a picture, making it more consistent in recognising faces behind FMs.

Issaoui and Selmi [19] proposed a Weighted Soft Discernibility Matrix with DL-driven FM Detection (WSDMDL-FMD) method by utilizing Mask Region-Based CNN (Mask R-CNN), extracting features with CNN optimized by Cuckoo Optimization Algorithm (COA), and classifying mask presence using the Weighted Soft Discernibility Matrix (WSDM) model. Sumathy et al. [20] developed a DL-based double generator network that utilizes the two-dimensional stationary wavelet transform (2D-SWT) model for image decomposition, the Haar cascade classifier for masked face biometric capture, and dual modules for edge generation and image reconstruction.

Karamizadeh, Shojae Chaeikar, and Salarian [21] developed a framework that integrates a convolutional (Conv.) model, namely Multi-task Cascaded Convolutional Networks (MTCNN) approach. The FaceNet with Attention Mechanisms (AMs) is also used for more discriminative facial embeddings, and an Adaptive Feature Fusion (AFF) module that uses contextual cues.

Kanavos et al. [22] introduced a system using a CNN trained on diverse mask-wearing conditions. Bhavani and Karthikeyan [23] developed an approach by utilizing the Improved Kuan Filter for image pre-processing, an Attention-Based Deep CNN (ADCNN) technique for feature extraction, an Improved Red Fox Optimizer (IRFO) for optimal feature selection, and an SVM-assisted ConvFaceNeXt (SVM_CFN) for final classification.

Nelson and Shaji [24] developed a model using Oriented Fast and Rotated Brief (ORB) with contrast alteration integrated with CNN for extraction, and a Generative Adversarial Network (GAN) optimized by the Search and Rescue-Sparrow Search Algorithm (SR-SSA) model for accurate occluded face recognition. Aly [25] presented an online educational platform that uses Residual Network 50 (ResNet50), the Convolutional Block Attention Module (CBAM), and Temporal Convolutional Networks (TCNs) for accurate recognition. VG, Kamalesh, and Apoorva [26] proposed a technique by employing an ensemble approach that integrates Histogram of Oriented Gradients (HOG) with an RF classifier. The existing studies exhibit various limitations, including occlusion severity, illumination shifts, pose variations, and low-resolution inputs. Few models exhibit limitations as they heavily depend on massive, domain-specific datasets, making them less adaptable when trained on limited or imbalanced data. Furthermore, approaches such as CNN-, SRC-, and GAN- lack an integrated mechanism for

handling both occlusion recovery and identity preservation simultaneously. Moreover, scalability and latency threats can be seen in real-time systems, namely CNNs or RF, when deployed on resource-constrained devices. Also, attention- or fusion-based methodologies illustrate weakness when masks cover major facial regions. Thus, the research gap is in developing an end-to-end framework that ensures high accuracy, resilience to occlusion and environmental discrepancies, efficient feature discrimination, and dependable recognition performance across diverse real-world scenarios.

3. Materials and Methods

This study proposes the MFRS-GCNMOA technique. The aim is to detect and recognize masked faces utilizing advanced models. To achieve that, the MFRS-GCNMOA model involves WF-based image pre-processing, feature extraction using ResNet152, a GCN-based classification model, SFOA for parameter tuning, and a decision-making process using the faster-RCNN model. Figure 1 depicts the flow of the MFRS-GCNMOA model.

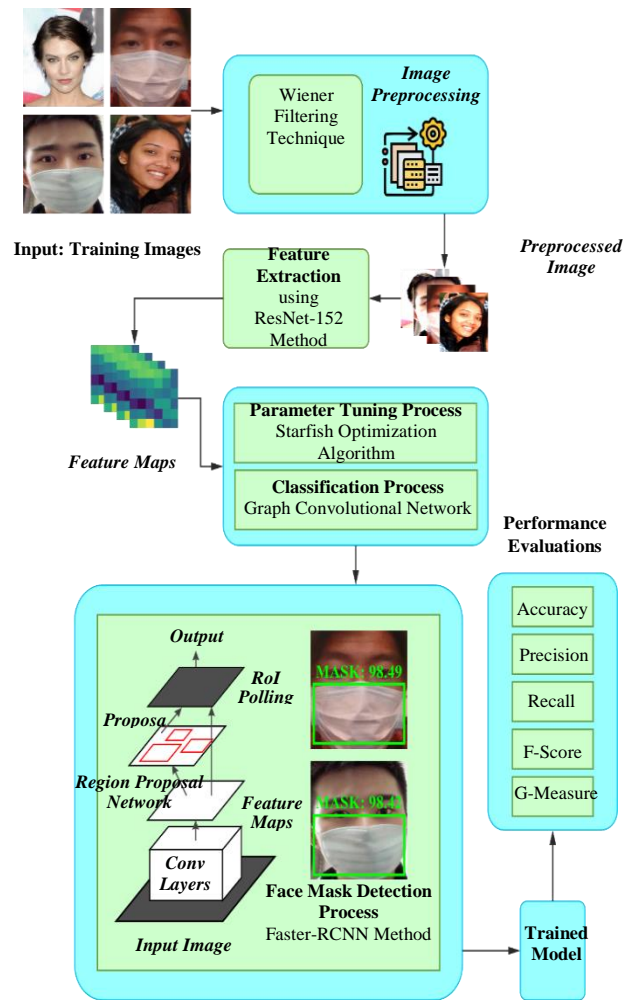


Fig. 1 Overall working flow of the MFRS-GCNMOA technique

3.1. Image Pre-Processing

This process is employed by using the WF method to eliminate the noise. WF functions as an adaptive model that accomplishes noise reduction estimation depending on local variance, while modifying its filtering procedure to match [27]. If the WF has a 5x5 window size, it strikes a better equilibrium between edge preservation and noise reduction. While utilised on Gaussian noise, the WF delivers exceptional performance and is helpful for different noise levels in Images—the filter model results in slight blurring of Image regions that should uphold their original sharpness.

$$h_{Wiener}(x, y) = \frac{Var(f_{local}(x, y))}{Var(f_{local}(x, y)) + \sigma^2} \quad (1)$$

3.2. ResNet-152-based Feature Extraction

For an effective feature extraction process, the MFRS-GCNMOA model utilises the ResNet-152 technique. This method is chosen owing to its deep framework and can manage the problem of vanishing gradients by using residual connections [28]. It acquires more intricate and abstract features, which are essential for differentiating subtle variances compared to CNN or standard Deep Networks. It contains a depth of 152 layers, which permits it to learn richer hierarchical representations, improving precision. The skip connections enhance the flow of the gradient and permit improved stability of training. Additionally, it verified effectiveness through different vision tasks, making it dependable for detection.

The well-known deep residual network ResNet-152 is implemented using the pre-trained method in DCNN. It is accountable for managing the issue of vanishing gradients. Subsequently, the ResNet152 output is transmitted to the SoftMax Classifier (SMC). The subsequent part encompasses the procedure of recognising and classifying features. The Convolution Layer (CL), Downsampling Layer (DSL), and Fully Connected (FC) layer are the most common layers that constitute DCNN. The depth of the DL approach is vital in achieving improved classifier performances. Once the CNN is made deeper, the accuracy of the network begins to slow down.

$$W(x) = K(x) + x \quad (2)$$

Now, $W(x)$ signifies a mapping function. Generally, SC is the identity mapping, resulting from bypassing the same layers; $K(x, G_i)$ denotes the representation of the residual mapping function.

$$Z = K(x, G_i) + x \quad (3)$$

In the CL of the ResNet model, 3x3 filtering is implemented, and the process of down-sampling is executed by a stride of 2.

$$u = \frac{1}{n} \sum_{i=1}^n [z \log(S_i) + (1 - z) \log(1 - S_i)] \quad (4)$$

Here, u denotes the loss function, n signifies the number of training samples, and S_i Depicts the output of SMC, a type of general Logistic Regression (LR) used with various classes.

$$S_i = \frac{e^{l_k}}{\sum_{j=1}^m e^{y_j}}, k = 1, \dots, m, y = y_1, \dots, y_m \quad (5)$$

While l and m represent the overall counts of neurons determined in the layer of output, l_k signifies the element of the input vector.

3.3. Classification using the GCN Model

Moreover, the GCN technique is deployed for classification purposes. In GCN, buses were deliberated as nodes and transmission lines as edges [29]. It contains three layers: input, output, and hidden. In graph $G = (N, E)$, E represents the edges among nodes, and N signifies the nodes.

3.3.1. Input Layer

The adjacency and feature matrix form GCN's input layer. The adjacency matrix depicts the connections among graph nodes, representing the transmission lines among buses.

$$Input = (X, A) \quad (6)$$

Here, X depicts a feature matrix. Likewise, n and d signify the count of nodes or buses and the input feature counts. A also has nxn dimensions that denote an adjacency matrix.

$$A_{ij} = A_{ji} \begin{cases} 0, i \neq j \\ 1, i = j \end{cases} \quad (7)$$

Where, A_{ij} signifies whether the node i_{th} connected with the node j_{th} .

3.3.2. Hidden Layer (HL)

To utilise the propagation rule, the HL of GCN gathers and sends node info to the succeeding layer. The layer-wise propagation rule of the i_{th} The node is given.

$$h_i^l = \sigma \left(\sum_{j=1}^N \bar{A}_{ij} \cdot w^l \cdot h_j^{l-1} + b^l \right) \quad (8)$$

$$\bar{A} = Q^{-\frac{1}{2}} A Q^{-\frac{1}{2}} \quad (9)$$

$$Q = \sum_{j=1}^N A_{ij} \quad (10)$$

Here, w^l signifies a trainable linear transformation of weights evaluated to decrease the loss function on each labelled data point, \bar{A} signifies the normalised adjacency matrix, b^l depicts a biased variable, σ indicates a non-linear activation function, h_j^l represents the i_{th} node features of l_{th} HL, and Q signify the input graph's degree matrix. Primarily, $h_i^0 = X$.

3.3.3. Output Layer

To eliminate the features from HL, the output layer creates the likelihood value of secured and insecure classes by utilising the softmax function.

3.4. SFOA-Based Parameter Tuning Model

Afterwards, the parameter tuning method is applied to SFOA to improve classification performance. Stimulated by the starfish's predatory behaviour inside the sea, the SFOA is separated into the initialisation, development, and exploration phases [30].

(1) Initialisation Phase:

In this phase, the starfish populace arbitrarily creates the location, and its formulation is as demonstrated:

$$X_{ij} = L_j + R \times (U_j - L_j), i = 1, 2, \dots, N \& j = 1, 2, \dots, M \quad (11)$$

Whereas X_{ij} Refers to the j th location of i th starfish, R

$$\begin{cases} Y_{i,p}(t) = X_{i,p}(t) + \alpha_1 [X_{best,p}(t) - X_{i,p}(t)] \cos \varphi, R \leq 0.5 \\ Y_{i,p}(t) = X_{i,p}(t) - \alpha_1 [X_{best,p}(t) - X_{i,p}(t)] \sin \varphi, R > 0.5 \\ \alpha_1 = 2(R - 1) \times \pi \\ \varphi = (\pi/2) \times (t/T_{max}) \end{cases} \quad (12)$$

Whereas $Y_{i,p}(t)$ characterises the location gained by the starfish, $X_{i,p}(t)$ symbolises the present starfish's location, $X_{best,p}(t)$ symbolises the p th size of the present optimal location, p is five arbitrarily chosen dimensions M , $\varphi \in$

indicates an arbitrary number in $[0, 1]$, U_j and L_j Specify the upper and lower boundaries, N denotes the count, and M indicates the problem size.

(2) Exploration Phase:

This starfish contains five arms. This novel searching type is presented in the exploration phase. The 5-dimensional searching model is incorporated with the 1D searching manner.

(1) When the optimiser problem dimension is more than 5, they move five arms to look for a meal.

$[0, \pi/2]$, and T_{max} refers to the maximal iteration counts.

(2) When the optimisation problem dimension is lower than 5, they utilise a 1D method for searching, and its mathematical representation is as demonstrated:

$$\begin{cases} Y_{i,p}(t) = EN \times X_{i,p}(t) + B \times [X_{y,p}(t) - X_{i,p}(t)] + C \times [X_{z,p}(t) - X_{i,p}(t)] \\ EN = (T_{max} - t)/(T_{max}) \cos \varphi \end{cases} \quad (13)$$

Whereas $X_{y,p}(t)$ and $X_{z,p}(t)$ represent p -dimensional locations of 2 starfish arbitrarily chosen in the populace, $C \in [-1, 1]$, and EN refers to the starfish's energy.

Here, R_1 and R_2 represent an arbitrary number in $[0, 1]$, and D_{m1} and D_{m2} denote arbitrarily chosen values in D_m .

(3) Development Phase:

In this phase, the starfish applied two strategies: regeneration and predation.

(2) Regeneration Approach: Once natural opponents catch the starfish, it will cut an arm to flee. Then, the regeneration tactic was performed in the final starfish within the populace.

(1) Predation Approach: The starfish utilises parallel bi-directional searching approaches using the information of another starfish and the optimal location of the present population.

$$Y_j(t) = \exp \left[\frac{-t \times N}{T_{max}} \right] X_j(t) \quad (16)$$

After the starfish's place surpasses the border, the location formulation is as demonstrated:

In the primary stage, the five distances between the optimal place and another starfish are measured. Then, two distances are arbitrarily chosen for validation to enhance the population of the starfish.

$$X_i(t+1) = \begin{cases} Y_i(t), l_b \leq Y_i(t) \leq u_b \\ l_b, Y_i(t) < l_b \\ u_b, Y_i(t) > u_b \end{cases} \quad (17)$$

$$D_m = [X_{best}(t) - X_{m_p}(t)], m = 1, 2, 3, 4, 5 \quad (14)$$

Whereas, D_m refers to the distance between the five global best starfish and another starfish, m_p Characterises five arbitrarily picked starfish, and the updated rule of all starfishes is as shown:

$$Y_i(t) = X_i(t) + R_1 D_{m1} + R_2 D_{m2} \quad (15)$$

To achieve enhanced classification performance, the SFOA originates a Fitness Function (FF). It governs a positive numeral to specify the enhanced candidate solution. The classifier error rate mitigation is measured as FF in Equation (18).

$$\begin{aligned} fitness(x_i) &= ClassifierErrorRate(x_i) \\ &= \frac{No. of misclassified samples}{Overall samples} \times 100 \end{aligned} \quad (18)$$

3.5. Face Mask Detection using Faster-RCNN Model

At last, the faster-RCNN method is employed for the FM detection process. Faster-RCNN is an expansion of the Fast-RCNN technique, which contains dual modules. The 1st module depends on the Region Proposal Network (RPN) that presents diverse areas [31]. The 2nd module is a detector that identifies various objects depending on the RPs eliminated by the 1st module.

3.5.1. RPN

RPN's input is an image dimension, and the outcomes have diverse RPs with a rectangular dimension, each with its own score. It generates a score for every region that indicates whether a region comprises an object or not. To create RPs, a smaller slide of the network is used to map the outcome in convolution feature mapping—an nxn spatial window acquired as input by a smaller network.

3.5.2. Anchors

At the position of every sliding window, many RPs were predicted concurrently, and for every position, the most probable proposal was depicted by k . Each k proposal is relative to k reference boxes known as anchors. Every anchor is connected with a scale and a ratio, both positioned at a sliding window.

3.5.3. Loss Function

By training RPN, dual classes are used to determine whether an object is present for every anchor.

$$L(\{p_j\}, \{t_j\}) = \frac{1}{N_{cls}} \sum_j L_{cls}(p_j, p_j^*) + \lambda \frac{1}{N_{reg}} \sum_j p_j^* L_{reg}(t_j, t_j^*) \quad (19)$$

Here, p_j Indicates the predicted likelihood or outcome scores of anchors, and mini-batch j depicts the anchor index for every anchor. If a positive anchor arises, p_j^* Depicts the ground truth as 1 and 0 if a negative comes. The four bounding box coordinates are displayed as t_j , whereas the ground truth coordinates connected with the positive anchor are indicated as t_j^* . The classification loss through dual classes was specified by L_{cls} and $L_{reg}(t_j, t_j^*) = R(t_j - t_j^*)$, which is utilised for regression loss here, where R indicates the loss function. The loss of regression is activated and depicted by $p_j^* L_{reg}$ for positive anchor ($p_j^* = 1$) only and disabled if ($p_j^* = 0$). The outcomes of the FC layer, such as reg and cls , are encompassed by $\{t_j\}$ and $\{p_j\}$. λ is a parameter balancing and standardised by N_{cls} and N_{reg} , subsequently. N_{cls} denotes the standardisation of the mini-batch parameter, and N_{reg} Depicts the standardisation parameters of the regression loss, equal to the counts of the anchor's position.

$$t_x = \frac{x - x_a}{w_a}, t_y = \frac{y - y}{h_a} \quad (20)$$

$$t_w = \log(w/w_a), t_h = \log(h - /h_a) \quad (21)$$

$$t^*x = (x^* - x_a)/w_a, t^*y = (y^* - y)/h_a \quad (22)$$

$$t^*w = \log(w^*/w_a), t^*h = \log(h^*/h_a) \quad (23)$$

Here, the box centre coordinates are depicted as x, w, y, h . The ground truth, predicted, and anchor bounding boxes are indicated as x^*, x, x_a . A similar case with y, w , and h . Particularly, x^*, w^*, y^*, h^* Signify the ground-truth of the box, and the width, height, and coordinates of the prediction box depict w, y, h , for the anchor box, which denotes x_a, w_a, y_a, h_a .

4. Performance Analysis

The performance of the MFRS-GCNMOA technique is investigated under the FM detection dataset [32]. It comprises 7,553 images, classified into dual class labels: With mask (3,725 images) and Without mask (3,828 images). The dataset is well balanced, with approximately equal representation of both classes, making it suited for training and assessing DL approaches for mask detection and FR tasks in computer vision. This dataset is effectually employed for emerging real-time monitoring systems in public spaces to ensure compliance with mask-wearing policies. Figure 2 represents the sample images. Figure 3 demonstrates the sample of the original and detected images.

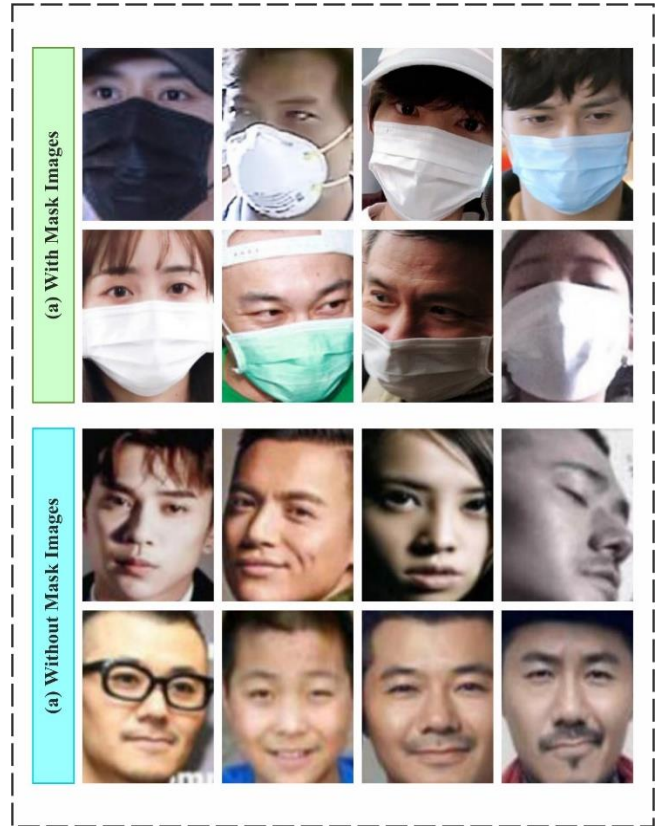


Fig. 2 Sample images: (a) With mask, and (b) Without mask.

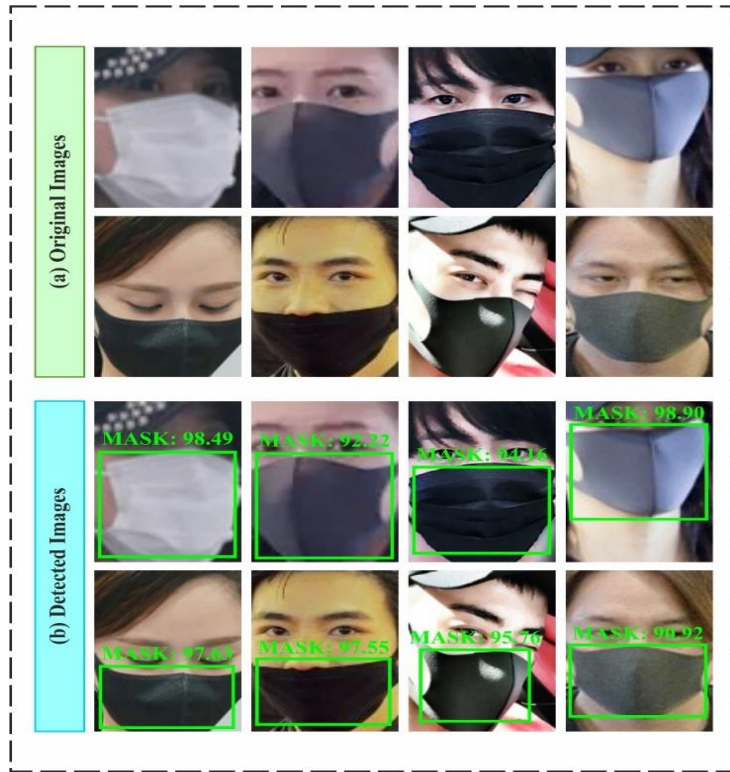


Fig. 3 Sample images of (a) Original image, and (b) Detected image

Figure 4 depicts the classifier performance of the MFRS-GCNMOA methodology. Figure 4(a) and 4(c) portray the confusion matrices with accurate classification of each class. Figure 4(b) shows the analysis of PR, representing the

maximum outcome for each class label. Finally, Figure 4(d) signifies the study of ROC, verifying capable solutions with superior ROC values for diverse classes.

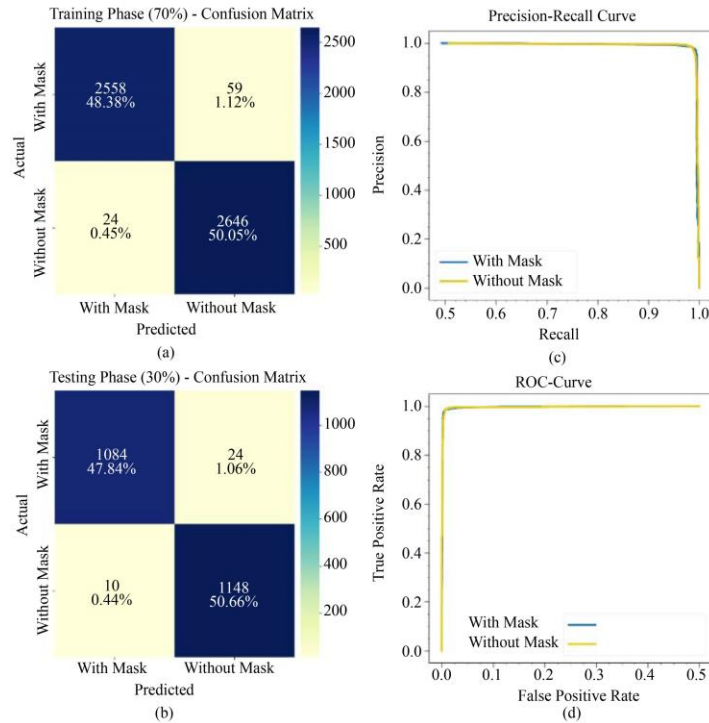


Fig. 4 Classifier outcome of MFRS-GCNMOA methodology (a), (c) Confusion matrix, and (b), (d) PR and ROC curves.

Table 1 and Figure 5 indicate the FM detection of the MFRS-GCNMOA method under 70:30. Under 70%TRPHE, the MFRS-GCNMOA approach reaches average $accu_r$, $preci_n$, $recal_l$, F_{Score} , and $G_{Measure}$ of 98.42%, 98.44%,

98.42%, 98.43%, and 98.43%, correspondingly. Moreover, on 30%TSPHE, the MFRS-GCNMOA approach accomplishes average $accu_r$, $preci_n$, $recal_l$, F_{Score} , and $G_{Measure}$ of 98.49%, 98.52%, 98.49%, 98.50%, and 98.50%, respectively.

Table 1. FM detection of the MFRS-GCNMOA approach under 70:30

Class Labels	$Accu_r$	$Preci_n$	$Recal_l$	F_{Score}	$G_{Measure}$
Training Phase (70%)					
With Mask	97.75	99.07	97.75	98.40	98.41
Without Mask	99.10	97.82	99.10	98.46	98.46
Average	98.42	98.44	98.42	98.43	98.43
Testing Phase (30%)					
With Mask	97.83	99.09	97.83	98.46	98.46
Without Mask	99.14	97.95	99.14	98.54	98.54
Average	98.49	98.52	98.49	98.50	98.50

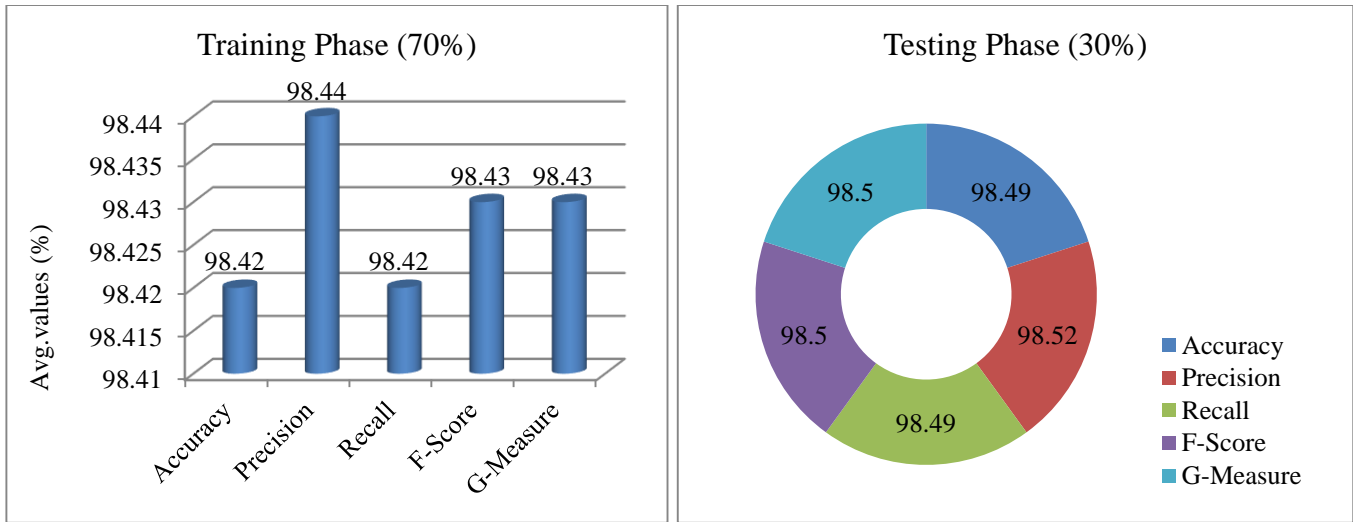


Fig. 5 Average values of MFRS-GCNMOA approach: (a) 70%, and (b) 30%.

Figure 6 reveals the Training (TRAN) and Validation (VALD) $accu_r$ Of the MFRS-GCNMOA model over 100 epochs. Both curves rise and converge, with VALD $accu_r$ Slightly higher than TRAN, illustrating the model learns effectively, generalizes well, and remains stable despite task difficulty.

Figure 7 portrays the TRAN and VALD loss of the MFRS-GCNMOA technique over 100 epochs. Both curves show a steady decline, with VALD loss slightly lower than TRAN loss, specifying effective learning, good generalization, and increasing stability.

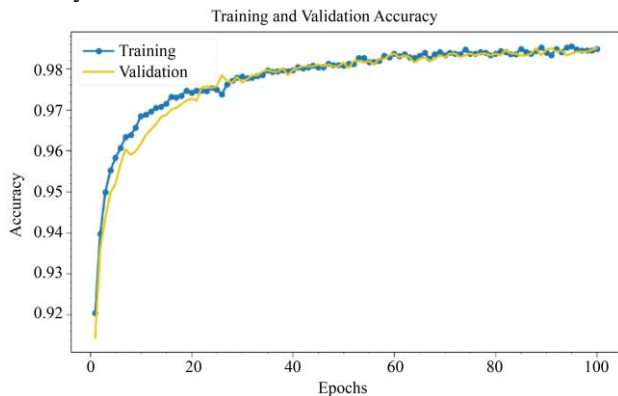


Fig. 6 $Accu_r$ Curve of the MFRS-GCNMOA technique

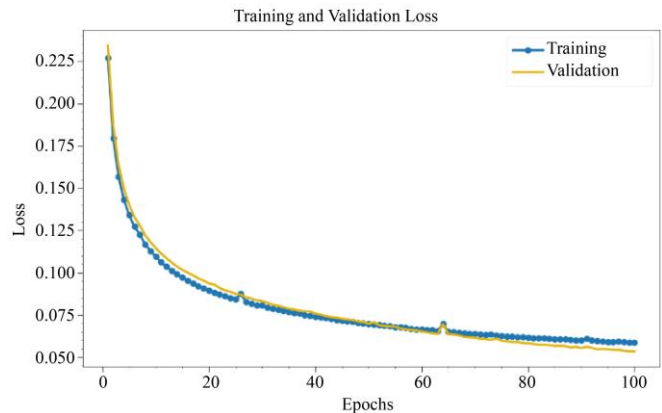


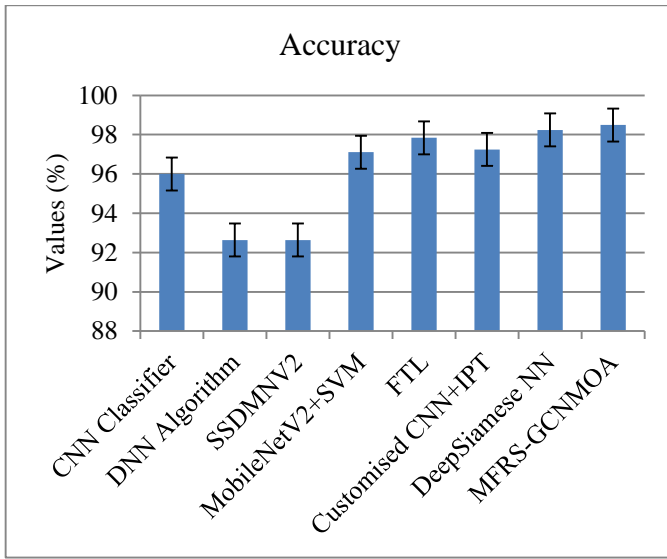
Fig. 7 Loss curve of MFRS-GCNMOA technique

To validate the greater outcome of the MFRS-GCNMOA methodology, a brief comparison analysis is formed in Table 2 and Figure 8 [5, 16]. The solution proved that the CNN, DNN, and SSDMNV2 have shown fewer outcomes. Meanwhile, the MobileNetV2+SVM, Fusion Transfer Learning (FTL), and Customised CNN+IPT approaches have tried to achieve somewhat nearer performances.

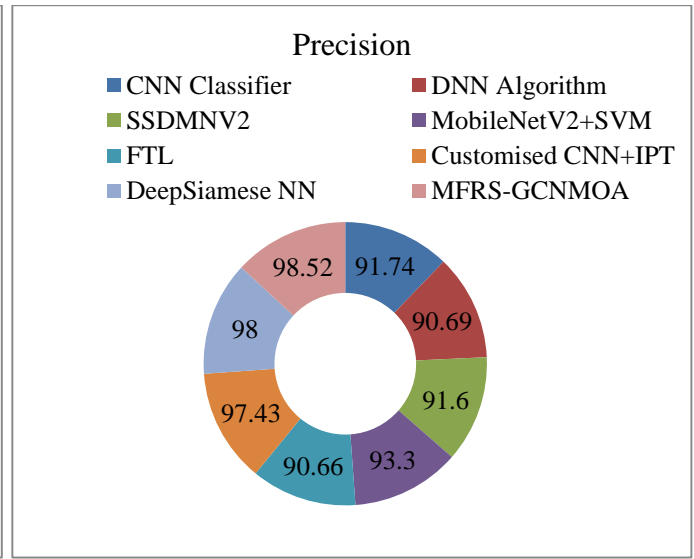
Additionally, the DeepSiamese NN technique has displayed a reasonable solution with $accu_r_y$ of 98.24%, $preci_n$ of 98.00%, $recal_l$ of 90.86%, and F_{score} Of 92.24%. Nevertheless, the MFRS-GCNMOA approach validates a promising outcome with $accu_r_y$ of 98.49%, $preci_n$ of 98.52%, $recal_l$ of 98.49%, and F_{score} of 98.50%.

Table 2. Comparative analysis of the MFRS-GCNMOA model with existing techniques

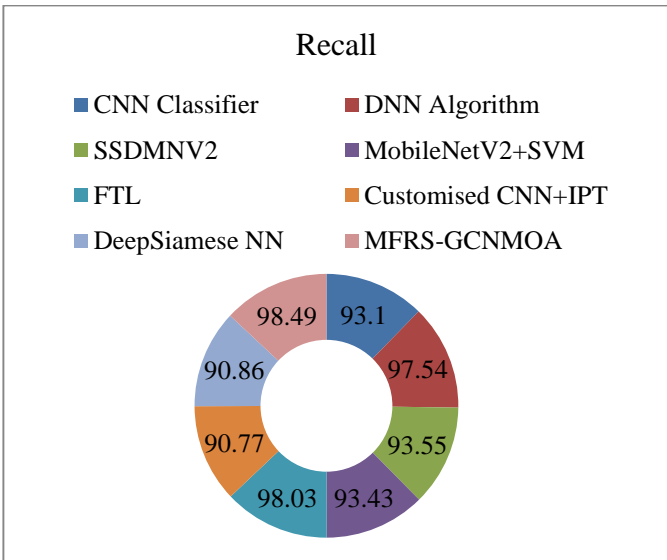
Techniques	$Accu_r_y$	$Preci_n$	$Recal_l$	F_{Score}
CNN Classifier	96.00	91.74	93.10	92.14
DNN Algorithm	92.64	90.69	97.54	92.67
SSDMNV2	92.64	91.60	93.55	96.96
MobileNetV2+SVM	97.11	93.30	93.43	92.13
FTL	97.84	90.66	98.03	97.71
Customised CNN+IPT	97.25	97.43	90.77	98.16
DeepSiamese NN	98.24	98.00	90.86	92.24
MFRS-GCNMOA	98.49	98.52	98.49	98.50



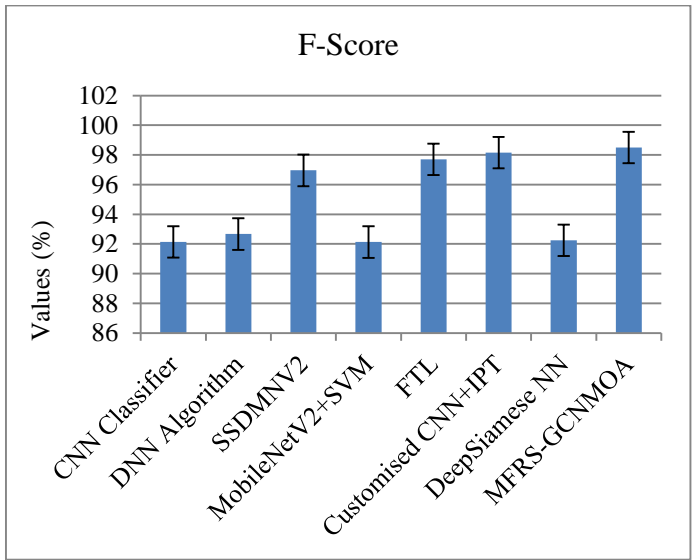
(a)



(b)



(c)



(d)

Fig. 8 Comparative analysis of MFRS-GCNMOA model with existing techniques

Table 3 and Figure 9 specify the comparison analysis of the MFRS-GCNMOA approach in terms of Execution Time (ET). The MFRS-GCNMOA approach presents a minimal ET of 8.82sec. Simultaneously, the existing models like CNN, DNN, SSDMNV2, MobileNetV2+SVM, FTL, Customized CNN+IPT, and DeepSiamese NN have accomplish superior ET of 16.28sec, 26.92sec, 16.77sec, 21.90sec, 11.65sec, 17.66sec, and 25.54sec, respectively.

Table 3. ET Outcome of MFRS-GCNMOA technique with recent models

Techniques	ET (sec)
CNN Classifier	16.28
DNN Algorithm	26.92
SSDMNV2	16.77
MobileNetV2+SVM	21.90
FTL	11.65
Customised CNN+IPT	17.66
DeepSiamese NN	25.54
MFRS-GCNMOA	8.82

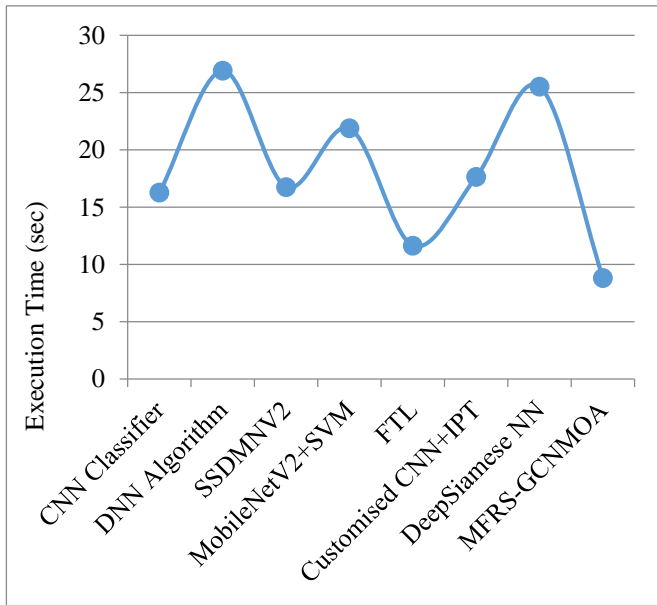


Fig. 9 ET outcome of MFRS-GCNMOA technique with recent models

Table 4 and Figure 10, the FR outcome of the MFRS-GCNMOA approach is clearly portrayed. The results showed that the MFRS-GCNMOA approach accomplishes better performance. Based on mAP@0.5, the MFRS-GCNMOA approach presents higher mAP@0.5 of 96.3% while the YOLOv3, Faster R-CNN, SE-YOLOv3, YOLOv5, FMDYolo, and AI-Yolo models have attained lesser mAP@0.5 of 88.5%, 78.1%, 89.0%, 91.2%, 66.4%, and 94.1%. In addition, based on IoU, the MFRS-GCNMOA technique gains a maximal IoU of 93.6% while the YOLOv3, Faster R-CNN, SE-YOLOv3, YOLOv5, FMDYolo, and AI-

Yolo models have attained a minimal IoU of 77.9%, 70.2%, 92.0%, 87.3%, 85.6%, and 70.8%.

Table 4. FR Outcome of MFRS-GCNMOA model with existing methods

Models	mAP@0.5	IoU (%)
YOLOv3	88.5	77.9
Faster R-CNN	78.1	70.2
SE-YOLOv3	89.0	92.0
YOLOv5	91.2	87.3
FMDYolo	66.4	85.6
AI-Yolo	94.1	70.8
MFRS-GCNMOA	96.3	93.6

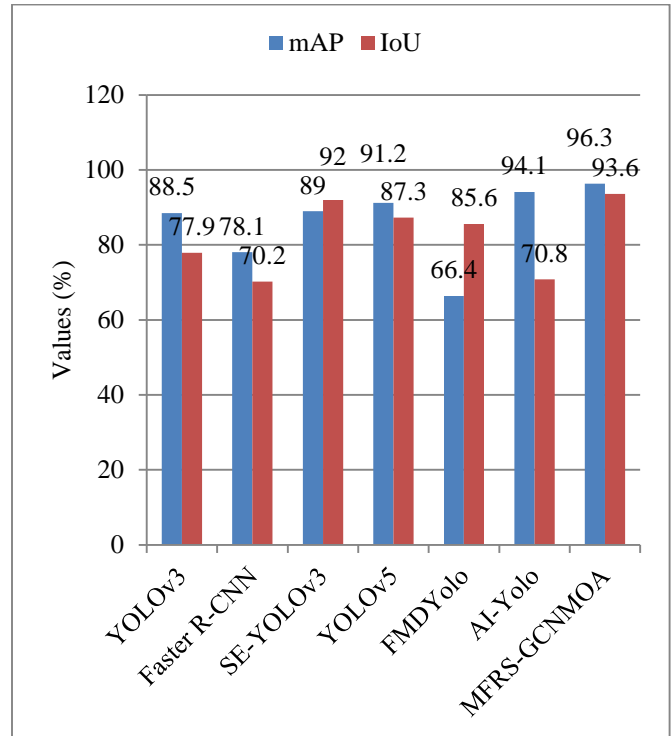


Fig. 10 FR Outcome of MFRS-GCNMOA model with existing methods

5. Conclusion

This study proposes the MFRS-GCNMOA technique. The image pre-processing stage is initially performed and employs the WF method to eliminate noise. For the feature extraction process, the MFRS-GCNMOA approach utilized the ResNet-152 model. In addition, the GCN technique was employed for classification purposes. Next, the parameter tuning was performed by implementing the SFOA technique.

Finally, the faster-RCNN method was used for FM detection. To show an improved performance of the presented MFRS-GCNMOA technique, a complete experimental study was conducted under the FM detection dataset. The comparison analysis of the MFRS-GCNMOA technique portrayed a superior accuracy value of 98.49% over existing models.

References

- [1] Bilal Saoud et al., "Review of Masked Face Recognition Based on Deep Learning," *Technologies*, vol. 13, no. 7, pp. 1-38, 2025. [[CrossRef](#)] [[Google Scholar](#)] [[Publisher Link](#)]
- [2] Rani Kurnia Putri, and Muhammad Athoillah, "Detection of Facial Mask using Deep Learning Classification Algorithm," *Journal of Data Science and Intelligent Systems*, vol. 2, no. 1, pp. 58-63, 2023. [[CrossRef](#)] [[Google Scholar](#)] [[Publisher Link](#)]
- [3] Sansiri Tarnpradab et al., "Real-Time Masked Face Recognition and Authentication with Convolutional Neural Networks on the Web Application," *Multimedia Tools and Applications*, vol. 84, pp. 22655-22679, 2025. [[CrossRef](#)] [[Google Scholar](#)] [[Publisher Link](#)]
- [4] Faezeh Mosayyebi, Hadi Seyedarabi, and Reza Afrouzian, "Gender Recognition in Masked Facial Images using EfficientNet and Transfer Learning Approach," *International Journal of Information Technology*, vol. 16, pp. 2693-2703, 2024. [[CrossRef](#)] [[Google Scholar](#)] [[Publisher Link](#)]
- [5] Mohamed Mahmoud, Mahmoud SalahEldin Kasem, and Hyun-Soo Kang, "A Comprehensive Survey of Masked Faces: Recognition, Detection, and Unmasking," *arXiv preprint*, pp. 1-33, 2024. [[CrossRef](#)] [[Google Scholar](#)] [[Publisher Link](#)]
- [6] Omer T. Hamajan, and Abbas M. Ali, "Masked Face Recognition using Deep Learning Models," *Zanco Journal of Pure and Applied Sciences*, vol. 36, no. 2, pp. 12-24, 2024. [[CrossRef](#)] [[Google Scholar](#)] [[Publisher Link](#)]
- [7] Mohamed Elhoseny et al., "Advanced Deep Learning for Masked Individual Surveillance," *International Journal of Cognitive Computing in Engineering*, vol. 5, pp. 406-415, 2024. [[CrossRef](#)] [[Google Scholar](#)] [[Publisher Link](#)]
- [8] Binay Kumar Pandey, Digvijay Pandey, and Mesfin Esayas Lelisho, "Face Mask Identification with Enhanced Cuckoo Optimisation and Deep Learning-Based Faster Regional Neural Network," *Scientific Reports*, vol. 14, pp. 1-18, 2024. [[CrossRef](#)] [[Google Scholar](#)] [[Publisher Link](#)]
- [9] Shivani Sharma et al., "Deep-MFR: A Deep Learning Ensemble Approach for Improved Masked Face Recognition," *International Conference on Advanced Network Technologies and Intelligent Computing*, Varanasi, India, pp. 212-228, 2025. [[CrossRef](#)] [[Google Scholar](#)] [[Publisher Link](#)]
- [10] Arpit Jain et al., "Deep Learning-Based Mask Identification System using ResNet Transfer Learning Architecture," *Computer Systems Science and Engineering*, vol. 48, no. 2, pp. 341-362, 2024. [[CrossRef](#)] [[Google Scholar](#)] [[Publisher Link](#)]
- [11] Aroobah Iftikhar, Arslan Shaukat, and Rimsha Tariq, "Masked Face Detection and Recognition Using a Unified Feature Extractor," *2024 5th International Conference on Advancements in Computational Sciences (ICACS)*, Lahore, Pakistan, pp. 1-6, 2024. [[CrossRef](#)] [[Google Scholar](#)] [[Publisher Link](#)]
- [12] Ashwan A. Abdulmunem, Noor D. Al-Shakarchy, and Mais Saad Safiq, "Deep Learning based Masked Face Recognition in the Era of the COVID-19 Pandemic," *International Journal of Electrical and Computer Engineering*, vol. 13, no. 2, pp. 1550-1559, 2023. [[CrossRef](#)] [[Google Scholar](#)] [[Publisher Link](#)]
- [13] Parul Dubey et al., "Enhanced IoT-Based Face Mask Detection Framework using Optimised Deep Learning Models: A Hybrid Approach with Adaptive Algorithms," *IEEE Access*, vol. 13, pp. 17325-17339, 2025. [[CrossRef](#)] [[Google Scholar](#)] [[Publisher Link](#)]
- [14] Ming Chun Yo, Siew Chin Chong, and Lee Ying Chong, "Sparse CNN: Leveraging Deep Learning and Sparse Representation for Masked Face Recognition," *International Journal of Information Technology*, vol. 17, pp. 4643-4658, 2025. [[CrossRef](#)] [[Google Scholar](#)] [[Publisher Link](#)]
- [15] Nay Kyi Tun, Aye Min Myat, "Proposed Activation Function Based Deep Learning Approach for Real-Time Face Mask Detection System," *International Journal of Electrical Engineering and Computer Science*, vol. 6, pp. 211-217, 2024. [[CrossRef](#)] [[Google Scholar](#)] [[Publisher Link](#)]
- [16] Hayat Al-Dmour et al., "Masked Face Detection and Recognition System based on Deep Learning Algorithms," *Journal of Advances in Information Technology*, vol. 14, no. 2, pp. 224-232, 2023. [[CrossRef](#)] [[Google Scholar](#)] [[Publisher Link](#)]
- [17] Akhil Kumar, "A Cascaded Deep-Learning-Based Model for Face Mask Detection," *Data Technologies and Applications*, vol. 57, no. 1, pp. 84-107, 2023. [[CrossRef](#)] [[Google Scholar](#)] [[Publisher Link](#)]
- [18] Mohammed Eman et al., "Innovative Hybrid Approach for Masked Face Recognition using Pretrained Mask Detection and Segmentation, Robust PCA, and KNN Classifier," *Sensors*, vol. 23, no. 15, pp. 1-20, 2023. [[CrossRef](#)] [[Google Scholar](#)] [[Publisher Link](#)]
- [19] Imène Issaou, and Afef Selmi, "Weighted Soft Discernibility Matrix with Deep Learning Assisted Face Mask Detection for Smart City Environment," *International Journal of Neutrosophic Science*, vol. 25, no. 1, pp. 179-189, 2025. [[CrossRef](#)] [[Google Scholar](#)] [[Publisher Link](#)]
- [20] G. Sumathy et al., "Real-Time Masked Face Recognition using Deep Learning-Based Double Generator Network," *Signal, Image and Video Processing*, vol. 18, pp. 325-334, 2024. [[CrossRef](#)] [[Google Scholar](#)] [[Publisher Link](#)]
- [21] Sasan Karamzadeh, Saman Shojae Chaeikar, and Hamidreza Salarian, "Combining MTCNN and Enhanced FaceNet with Adaptive Feature Fusion for Robust Face Recognition," *Technologies*, vol. 13, no. 10, pp. 1-25, 2025. [[CrossRef](#)] [[Google Scholar](#)] [[Publisher Link](#)]
- [22] Athanasios Kanavos et al., "Real-Time Detection of Face Mask Usage Using Convolutional Neural Networks," *Computers*, vol. 13, no. 7, pp. 1-21, 2024. [[CrossRef](#)] [[Google Scholar](#)] [[Publisher Link](#)]

- [23] Siriki Atchuta Bhavani, and C. Karthikeyan, “An Attention Based Deep Learning with Effective SVM-ConvFaceNeXt Model for Face Recognition in Unconstrained Environment,” *Signal, Image and Video Processing*, vol. 19, 2025. [[CrossRef](#)] [[Google Scholar](#)] [[Publisher Link](#)]
- [24] Abhilash Nelson, and R.S. Shaji, “A Novel Occluded Face Detection Approach using Enhanced ORB and Optimized GAN,” *International Journal of Wavelets, Multiresolution and Information Processing*, vol. 22, no. 2, 2024. [[CrossRef](#)] [[Google Scholar](#)] [[Publisher Link](#)]
- [25] Mohammed Aly, “Revolutionizing Online Education: Advanced Facial Expression Recognition for Real-Time Student Progress Tracking via Deep Learning Model,” *Multimedia Tools and Applications*, vol. 84, pp. 12575-12614, 2025. [[CrossRef](#)] [[Google Scholar](#)] [[Publisher Link](#)]
- [26] V.G. Manjunatha Guru, V.N. Kamalesh, and K.B. Apoorva, “An Ensemble Learning Based Approach for Real-Time Face Mask Detection,” *International Journal of Scientific Research in Computer Science and Engineering*, vol. 13, no. 3, pp. 8-13, 2024. [[Google Scholar](#)] [[Publisher Link](#)]
- [27] Mst Jannatul Kobra et al., “Effectiveness of Fourier, Wiener, Bilateral, and CLAHE Denoising Methods for CT Scan Image Noise Reduction,” *Scientific Journal of Engineering Research*, vol. 1, no. 3, pp. 96-108, 2025. [[CrossRef](#)] [[Google Scholar](#)] [[Publisher Link](#)]
- [28] Abrar Almjally, and Wafa Sulaiman Almkadi, “Deep Computer Vision with Artificial Intelligence Based sign Language Recognition to Assist Hearing and Speech-Impaired Individuals,” *Scientific Reports*, vol. 15, pp. 1-18, 2025. [[CrossRef](#)] [[Google Scholar](#)] [[Publisher Link](#)]
- [29] Sasan Azad, and Mohammad Taghi Ameli, “An Imbalanced Deep Learning Framework for Pre-Fault Flexible Multi-Zone Dynamic Security Assessment via Transfer Learning Based Graph Convolutional Network,” *Results in Engineering*, vol. 25, pp. 1-15, 2025. [[CrossRef](#)] [[Google Scholar](#)] [[Publisher Link](#)]
- [30] Guangjian Zhang, Shilun Ma, and Xulong Wang, “Fault Diagnosis of a Bogie Gearbox Based on Pied Kingfisher Optimizer-Improved Complete Ensemble Empirical Mode Decomposition with Adaptive Noise, Improved Multi-Scale Weighted Permutation Entropy, and Starfish Optimization Algorithm–Least-Squares Support Vector Machine,” *Entropy*, vol. 27, no. 9, pp. 1-28, 2025. [[CrossRef](#)] [[Google Scholar](#)] [[Publisher Link](#)]
- [31] Sohaib Asif et al., “Real-Time Face Mask Detection System Using Transfer Learning with Faster-RCNN in the Era of the COVID-19 Pandemic,” *2021 4th International Conference on Artificial Intelligence and Big Data (ICAIBD)*, Chengdu, China, pp. 70-75, 2021. [[CrossRef](#)] [[Google Scholar](#)] [[Publisher Link](#)]
- [32] Face Mask Detection Dataset, Kaggle. [Online]. Available: <https://www.kaggle.com/datasets/omkargurav/face-mask-dataset>